Earthquakes and Structures, *Vol. 16, No. 3 (2019) 311-320*
DOI: https://doi.org/10.12989/eas.2019.16.3.311

Estimation of structural dynamic characteristics of the Egyptian Obelisk of Theodosius

Özden Saygılı*

Department of Civil Engineering, Yeditepe University, 26 Agustos Campus, Kayisdagi St., 34755, Atasehir, Istanbul, Turkey

(Received August 2, 2018, Revised January 25, 2019, Accepted January 27, 2019)

Abstract. Obelisks are historical monuments. There are several obelisks dating from ancient Egyptian period, located around various parts of the world. The city of Istanbul is a home to the Obelisk of Theodosius at the Hippodrome. Due to the expectation of a large event in the near future, the evaluation of seismic response of the Obelisk gets importance. Therefore, in this study structural dynamic behavior of the Obelisk was investigated using discrete element approach. Nonlinear dynamic analyses were performed using real and synthetic time series. Real and synthetic ground motions analyzed from this study seems consistent with the earthquake hazard levels that would be expected at the site of the Obelisk in the occurrence of an event of moment magnitude above 7.0 near Istanbul. Results are evaluated in terms of variation of displacement, relative displacement of adjacent blocks, normal stress and shear stress in time.

Keywords: obelisk; discrete element modelling; nonlinear dynamic analysis

1. Introduction

Obelisks are historical monuments with a high, four-sided shape that taper into a pyramid at the top. There are several obelisks dating from ancient Egyptian period, located around various parts of the world. The Obelisk of Thutmose III at the Hippodrome of Istanbul is a monument brought from Egypt by the Roman emperor Theodosius I. It was originally made for Thutmose III, who ruled Egypt from 1479 to 1425. A sixth-century chronicler, Marcellinus Comes, states that the monument was erected in 390 CE. Therefore, the Obelisk was almost two millennia old already when it was placed at the Hippodrome. The Obelisk of Theodosius bears hieroglyphic inscriptions on all sides is of red granite from Aswan in Southern Egypt. A part of the Obelisk was missing (Engelbach 1923, Safran 1993, Klemm and Klemm 2008, Kelany *et al*. 2009). Before the lower part was damaged from transportation or re-erection, it was approximately 34.9 m tall by now 19.5 m. The Obelisk remain standing on four bronze cubes rest on a marble pedestal (Fig. 1).

Looking at the tectonic and seismic structure of the Marmara region, available tectonic and geologic studies (Nakano *et al*. 2015, Polat *et al*. 2016) indicated that the North Anatolian Fault (NAF) is one of the major continental transform faults in the world. The right-lateral, the almost purely strike-slip tectonic regime that characterizes the NAF over its eastern portion from the Karliova Triple Junction (KTJ) splays in the Sea of Marmara region into three major fault branches, the Northern, the Middle and the Southern strands (Barka 1992). Throughout history, many devastating earthquakes such as 1509, 1766, 1912 and 1999 caused by the NAF occurred in this region, particularly the megalopolis of Istanbul.

Fig. 1 Image of the Obelisk of Theodosius

It is worth pointing out that the Obelisk did not collapse or suffer any significant damage from devastating earthquakes, which caused to moderate and heavy damages to most of the historical structures. The İstanbul faces a significant earthquake hazard with the probability of exceedance 41±14% in the next 30 years for an event of moment magnitude above 7.0 (Parsons, 2004). There is a scarcity of information regarding the seismic behavior of the Obelisk of Theodosius. This study is thus aimed to investigate the structural dynamic behavior of the Obelisk of Theodosius. Discrete Element Approach (DEA) is utilized to create the numerical model. Nonlinear dynamic analyses were performed under real and synthetic time series using explicit integration method that assumes a

*Corresponding author, Assistant Professor
E-mail: ozden.saygili@yeditepe.edu.tr

Copyright © 2019 Techno-Press, Ltd.

ISSN: 2092-7614 (Print), 2092-7622 (Online)

linear change in displacement over each time step.

2. Layout and material properties of the obelisk

Electronic distance measuring instrument of a Total Station device was used to determine the present dimensions of the obelisk. In this case, accuracy is especially very important in Total Station device to record and calculate data. The instrument placed on a stable ground for the tripod feet at the site. It was centered precisely over the ground point by shifting the tribrach on the tripod plate until the required accuracy was achieved. Horizontal and vertical measurement data in reference to a target point were stored in a memory card. The file was structured in three columns with the *x*, *y* and *z* coordinates of the 58 number of points scanned. Scanned data was used to create the numerical model of the Obelisk. The existing height of the Obelisk is 19.46 m including the pyramidon part at the top. The taper part is 2.67 m and dimensions of pyramidon base are 1.67 m and 1.64 m. The base of the Obelisk resting dimensions are 2.01 m and 1.96 m. The Obelisk stands on four bronze cubes with an approximately dimensions in 0.48 m× 0.50 m×0.49 m. The upper part of the marble pedestal standing on porphyry cubes has approximately 2.35 m height and resting dimensions are 3.02 m and 2.68 m. The porphyry cubes are approximately in dimensions of 0.55 m×0.56 m×0.55 m. The lower part height of the marble pedestal is 1.86 m and base sides are 3.58 m and 3.73. The total height of the Obelisk including marble pedestal and stone masonry is approximately 24.77 m. As looking at previous studies, there are several historic, archeological and numerical studies were performed to investigate the material characteristics of obelisks, red Aswan granite, marble, stone and bronze used as a construction material in ancient Egyptian, Roman, Byzantine, and Ottoman empires (National Research Council 1982, Vasconcelos 2005, Sadan *et al.* 2007, Taliercio *et al.* 2007, Klemm and Klemm 2008, Ludovico-Marques 2008, Kelany *et al.* 2009, Klemm and Klemm 2009, Abdel-Gawwad *et. al* 2011, Borghi *et al.* 2011, Bongiovanni *et al* 2011, Borghi *et al.* 2015, Bilen *et al.* 2016, Arslan 2016, Waters 2016, Darwish and Rashwan 2018). Most of these studies emphasized the material properties of obelisks, bronze and marble based on experimental data. The Obelisk of Theodosius have traces of damage to the bronze cubes, porphyry cubes and marble pedestal perhaps from earthquakes or from other natural disasters. The average mechanical properties of the Obelisk were determined using information inferred from previous studies mentioned above and considering the obvious damages. In this study adopted mechanical properties are given in Table 1.

Table 1 Mechanical properties of the Obelisk

Material Property	Obelisk	Marble	Bronze	Stone Masonry
Density (10^3 kg/m^3)	2.54	2.75	8.30	2.04
Elastic Modulus (kPa)	3.92×10^6	70×10^6	900×10^5	13×10^6
Tensile Strength (kPa)	5.09×10^4	125	125×10^3	20×10^2
Compressive Strength (kPa)	2.14×10^5	12×10^4	315×10^3	36×10^3

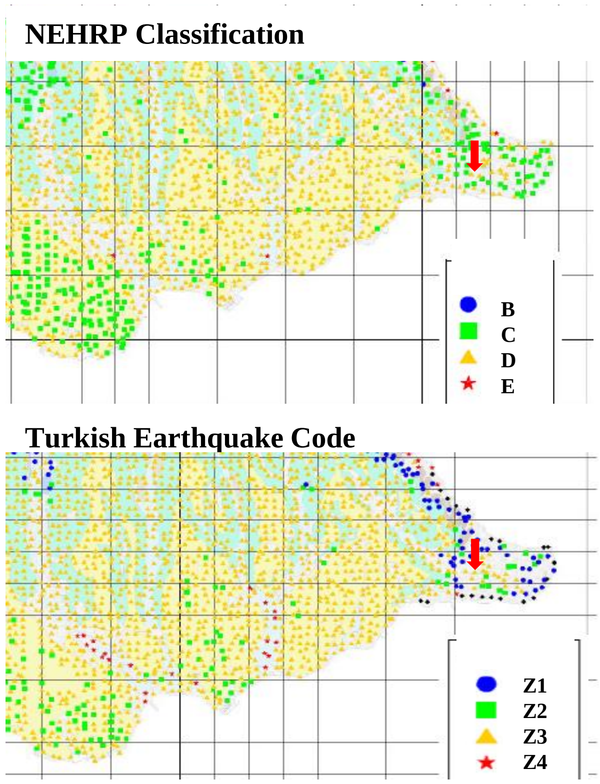

Fig. 2 Site Classification according to Turkish Earthquake Code and NEHRP (IMM 2007)

3. Ground motion selection

Synthetic and real ground motions were used to investigate the structural performance of the Obelisk. Four types of ground shaking level given in Turkish Structure Seismic Code 2018 were taken into consideration in creating synthetic time series. First earthquake ground motion level has a 2% probability to be exceeded in 50 years. Return period of this ground shaking is approximately 2475 years. Second earthquake ground motion level has a 10% probability to be exceeded in 50 years. Return period of this ground shaking is approximately 475 years. Third earthquake ground motion level having a 50% probability to be exceeded in 50 years with a return period of 72 years. Fourth ground motion level has a 50% probability to be exceeded in 68 years. Return period of this ground shaking is approximately 43 years. For each level 3 artificial ground motion compatible with design response spectrum were simulated using SeismoArtif software. To create artificial time series shear wave velocity down to 30 m depth and soil classification were determined using seismic microzonation maps arranged integrated use of all geophysical and geotechnical data prepared by the Istanbul Metropolitan Municipality (IMM) in the scope of “Geological-Geotechnical Study Report According to The Construction Plans as a Result of Settlement Purposed Microzonation Works” completed in 2007 (Fig. 2 and Fig.

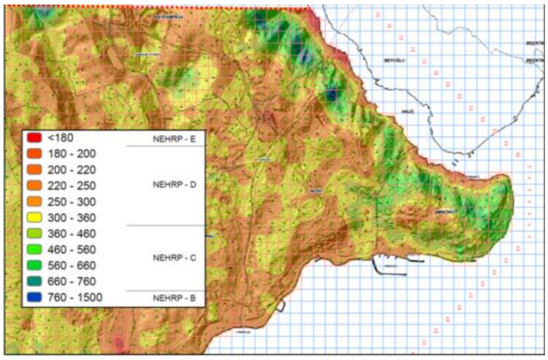

Fig. 3 Contour line map of the Shear Wave Velocity (IMM 2007)

Table 2 Synthetic ground motions

Earthquake Ground Motion Level 1			
Synthetic Ground Motion	SGM 1	SGM 2	SGM 3
PGA (g)	0.676	0.677	0.677
PGV (cm/s)	71.307	72.407	79.515
Earthquake Ground Motion Level 2			
Synthetic Ground Motion	SGM 1	SGM 2	SGM 3
PGA (g)	0.399	0.399	0.399
PGV (cm/s)	55.915	45.067	42.716
Earthquake Ground Motion Level 3			
Synthetic Ground Motion	SGM 1	SGM 2	SGM 3
PGA (g)	0.167	0.167	0.167
PGV (cm/s)	17.188	17.313	19.819
Earthquake Ground Motion Level 4			
Synthetic Ground Motion	SGM 1	SGM 2	SGM 3
PGA (g)	0.109	0.109	0.109
PGV (cm/s)	12.38	14.993	12.93

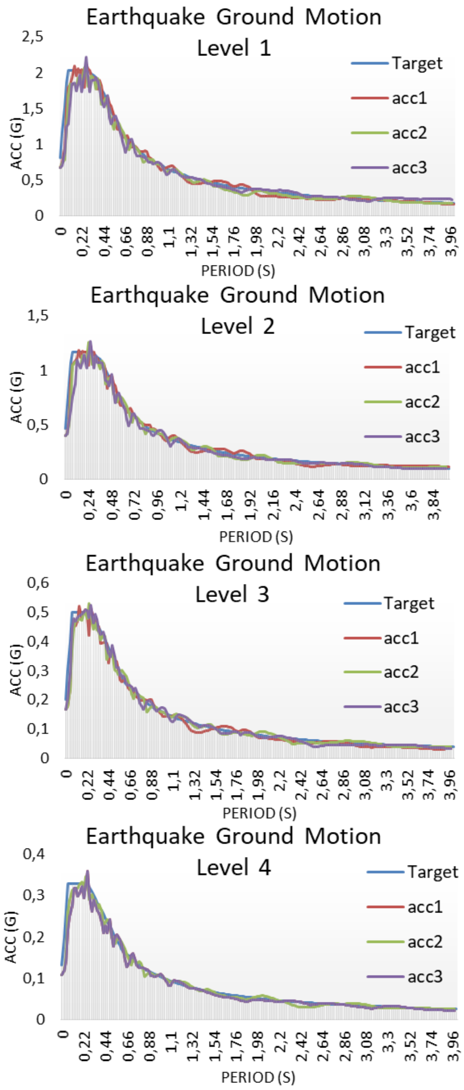

Fig. 4 Synthetic acceleration response spectrum and target response spectrum for four level of earthquake ground motion

3). The distance between the main event and the Obelisk is approximately 75 km. Peak ground acceleration (PGA) and peak ground velocity (PGV) of the synthetic motions are given in Table 2. Comparison of synthetic acceleration response spectrum and target response spectrum for each level are shown in Fig. 4.

In addition to synthetic ground motions, accelerograms recorded during real earthquakes were used as an input data. Real earthquakes are downloaded from ground PEER NGA strong motion database which includes a very large dataset of ground motions recorded in the worldwide shallow crustal earthquakes particularly in active tectonic regimes. The ground motion time histories were selected based on earthquake magnitude, rupture, focal mechanism, shear wave velocity and site classification. In terms of real earthquakes the numerical model of the Obelisk subjected to 1999, Kocaeli Turkey, 1999 Düzce Turkey, earthquakes in three orthogonal direction.

The 1999 Kocaeli, Turkey earthquake (magnitude 7.51) was associated with about 120 km rupture on the 1300 km long right lateral strike slip North Anatolian fault. The slip was typically 2.5 to 4.5 m, reaching a maximum of approximately 5 m at a location about 30 km to the east of the epicentre. The 1999 Düzce, Turkey earthquake (magnitude 7.14) is associated with Düzce Fault that joint to the North Anatolian fault system. Düzce earthquake produced a surface fault rupture of approximately 40 km (Erdik 2000).

Apart from these 2010 Darfield New Zealand, earthquake was used by ground motion scaling to match a target design spectrum of ground motion level 1. The 2010 Darfield, New Zealand earthquake (magnitude 7.0) was associated with the strike slip Greendale Fault. The motion produced about 29.5 km long, 30 to 300-m-wide zone of ground surface rupture (Quigley *et al*. 2012). The PGA of the 1999 Kocaeli Earthquake in 00, 90 and UP component are 0.1618 g, 0.1881 g and 0.1330 g, respectively. The earthquake has maximum PGV in 90 component with 0.1917 m/s. For the 1999 Düzce Earthquake, PGAs are 0.1367 g, 0.1524 g, 0.1010 g and PGV values are 0.1031 m/s, 0.1286 m/s, 0.0887 m/s in EW, NS and UP component, respectively.

For the 2010 Darfield New Zealand Earthquake, PGAs are 0.7645 g, 0.7080 g, 1.2498 g and PGV values are 1.0029 m/s, 1.1604 m/s, 0.3827 m/s in N55W, S55W and

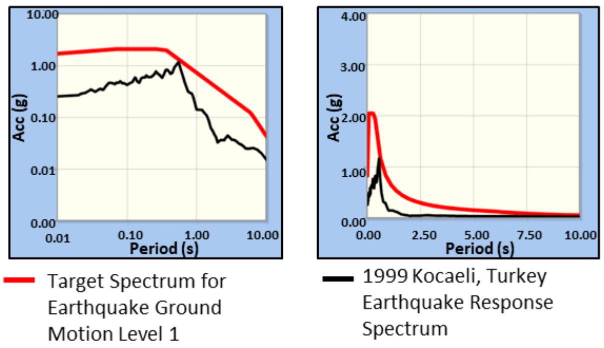

Fig. 5 The 1999 Kocaeli, Turkey Earthquake Spectrum and Target Spectrum of Earthquake Ground Motion Level 1 on loglog and linear plots

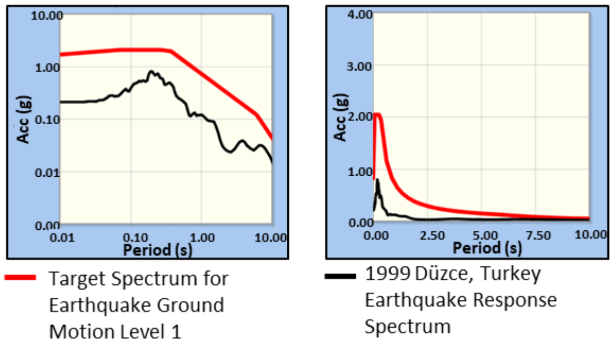

Fig. 6 The 1999 Düzce, Turkey Earthquake Spectrum and Target Spectrum for Earthquake Ground Motion Level 1 on loglog and linear plots

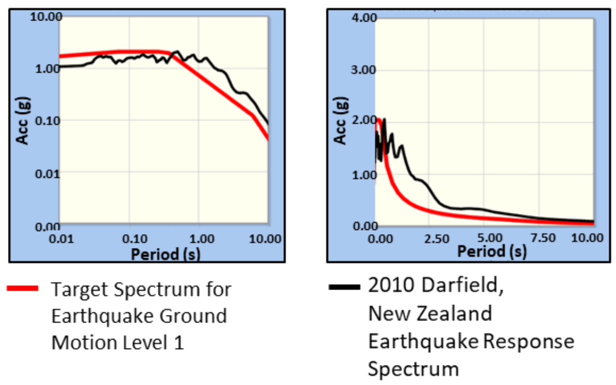

Fig. 7 The 2010 Darfield, New Zealand Earthquake Spectrum and Target Spectrum for Earthquake Ground Motion Level 1 on loglog and linear plots

UP component, respectively. Here, the response spectrums of Kocaeli, Düzce and Darfield earthquakes are compared with respect to target spectrum for earthquake ground motion level 1 on loglog and linear plots are given in Figs. 5 to 7.

4. Discrete element modeling

DEA was adopted to create the numerical model of the Obelisk which is a way to simulate the mechanical response of systems composed of discrete blocks or particles

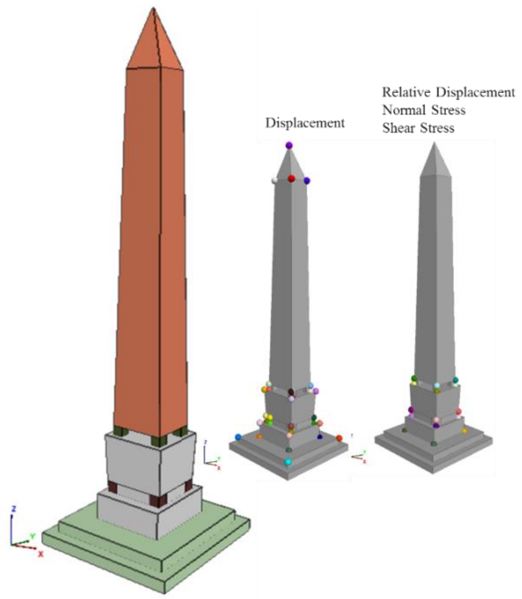

Fig. 8 Numerical model of the Obelisk and history locations

(Cundall and Strack 1979). This methodology is based on finite displacements and rotations of discrete bodies and this methodology allows to recognize new contacts automatically as the calculation progresses (Cundall and Hart 1992). Discrete element method (DEM) is getting more attention as an effective methodology (Mehrotra *et al.* 2015, Lemos *et al.* 2015, Çaktı *et al.* 2016, Pulatsu *et al.* 2016). Three dimensional distinct element code (3DEC) was used. The theory behind the 3DEC is based on discontinuous analysis techniques. The major elements of the formulation of the 3DEC are the scheme for contact detection and representation in three-dimensions, and the mechanical calculations for motion and interaction in three-dimensions (Itasca 2016). 11 rigid blocks were created. Each block touches a data element which can be considered as a physical contact between the two blocks. Deformability takes place at these contacts contains mechanical characteristics of friction, shear stiffness, normal stiffness, cohesion and tension. At the joints, between obelisk and bronze cubes, normal and shear joint stiffness parameters are 1.14 GPa/m and 0.46 GPa/m respectively. Another issue is the boundary conditions. The base of the obelisk was considered as completely constrained. The numerical model of Obelisk subjected to dynamic excitation in the elastic range to calculate the natural frequencies and modes of vibration. 66 stiffness equations were solved using explicit time-marching scheme for 11 rigid blocks and deformable contacts. Vector iteration procedure was applied to calculate the eigenvalues. The calculated natural frequency for first bending mode of vibration, second bending mode of vibration and first torsional mode of vibration is 0.886 Hz, 9.304 Hz and 10.75 Hz, respectively. For the dynamic analyses, mass proportional damping was used which applies a force that proportional to absolute velocity and mass in the direction opposite to the velocity (Itasca 2016). At the total of 48 points in the numerical model variation of the displacement and velocity in time were monitored during the dynamic analyses. At the total of 20 points on the numerical model relative displacements of adjacent blocks, change of normal stress and shear stress in time were also monitored. History locations are indicated in Fig. 8.

Dynamic input data were applied as the history of velocity. For the simulated ground motions acceleration histories were integrated numerically to produce a velocity history for 3DEC. Simulated velocity ground motions were applied in x direction. For real earthquakes velocity time histories were downloaded from PEER NGA Database. The numerical model of the Obelisk subjected to three orthogonal velocity ground motion data of the 1999 Kocaeli, Turkey earthquake, the 1999 Düzce, Turkey earthquake and the 2010 Darfield, New Zealand earthquake.

5. Nonlinear dynamic analyses

It is difficult to determine friction angle between the Obelisk and bronze cube. Thus in this study dynamic nonlinear analyses were performed for different friction angles of 25, 30, 35 and 40 in degrees. Three synthetic earthquakes created for each level of ground motion were given in Turkish Structure Seismic Code in 2018. Each artificial velocity data are thus applied in *x* direction. Maximum displacement at the top of the Obelisk in terms of different friction angle under three synthetic ground motion (SGM) is illustrated in Fig. 9. Additionally, time varying relative displacement histories of adjacent blocks for varying friction angle at the contact points between the Obelisk and bronze cubes were monitored. Under synthetic ground motions, highest relative displacement occurs between the Obelisk and bronze cubes. The maximum relative displacement values occurred at Joint 1 in terms of different friction angles under three synthetic ground motion is shown in Fig. 10.

At the earthquake ground motion level 4, the maximum displacement in the top of the Obelisk varies between 13 cm and 14 cm under the first SGM. At the second SGM, the observed maximum top displacement is between 15 cm and 16 cm which is very close to response under the SGM 3. At the earthquake ground motion level 3, the Obelisk experienced the maximum top displacement (0.37 cm) under the SGM 3 applied in different friction values. In addition to these, at the ground motion level 2, the maximum top displacement for four friction angle varies between 0.58-0.71 cm, 0.48-0.54 cm and 0.70-0.74 cm under SGM 1, SGM 2 and SGM 3, respectively.

The responses of the earthquake ground motion level 2, 3 and 4 show that the Obelisk experienced the top displacement in the same range for different friction values without necessarily exciting relative displacement. The maximum top displacement at the earthquake ground motion level 1 takes place under three synthetic ground motion for friction value of 40. At the ground motion level 2, 3 and 4, it is evident that the maximum relative displacement at the contacts are approximately in the same range for each synthetic ground motion. Under the ground motion level 1 that has a 2% probability to be exceeded in 50 years with a return period of 2475 years, the Obelisk experienced the highest maximum relative displacement (8.1 cm) at the SGM 1 applied in terms of friction angle 40.

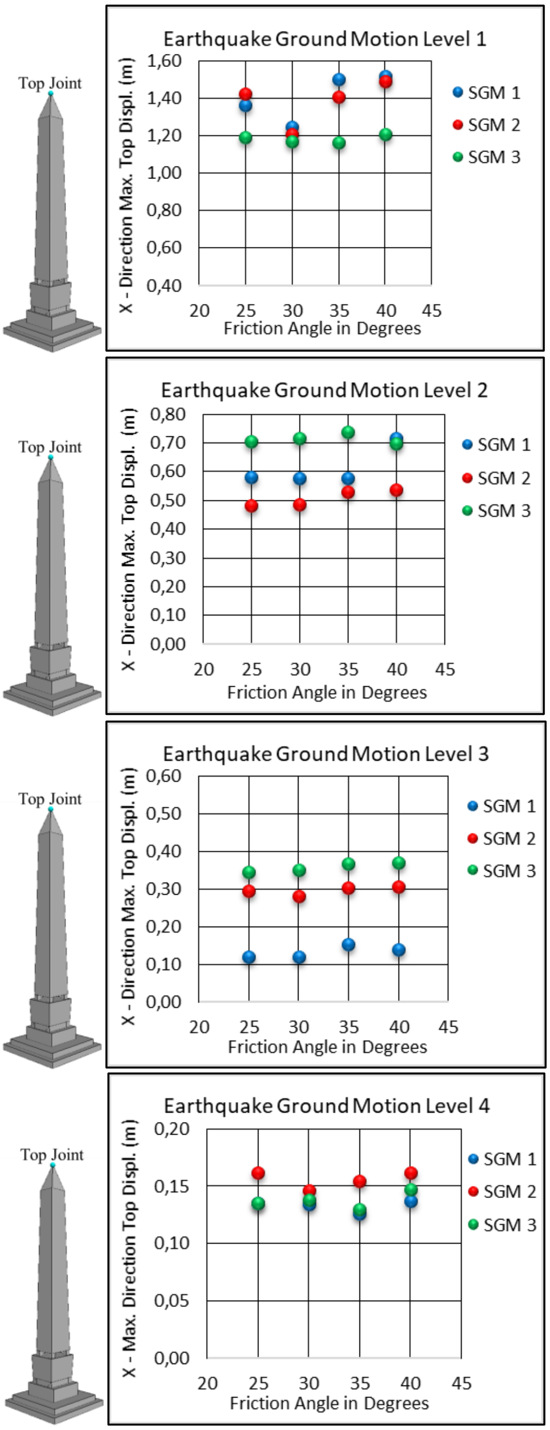

Fig. 9 The maximum displacement at the top of the Obelisk calculated in terms of different friction angles under the three synthetic ground motion (SGM)

The numerical model of the Obelisk subjected to ground motion data of the 1999 Kocaeli, Turkey earthquake, the 1999 Düzce, Turkey earthquake and 2010 Darfield, New Zealand earthquake. Dynamic nonlinear analyses were performed under the three orthogonal seismic wave components of the real earthquakes listed above.

Under seismic excitations, time-varying displacement and relative displacement histories of adjacent blocks for varying friction angles at the contact points between the

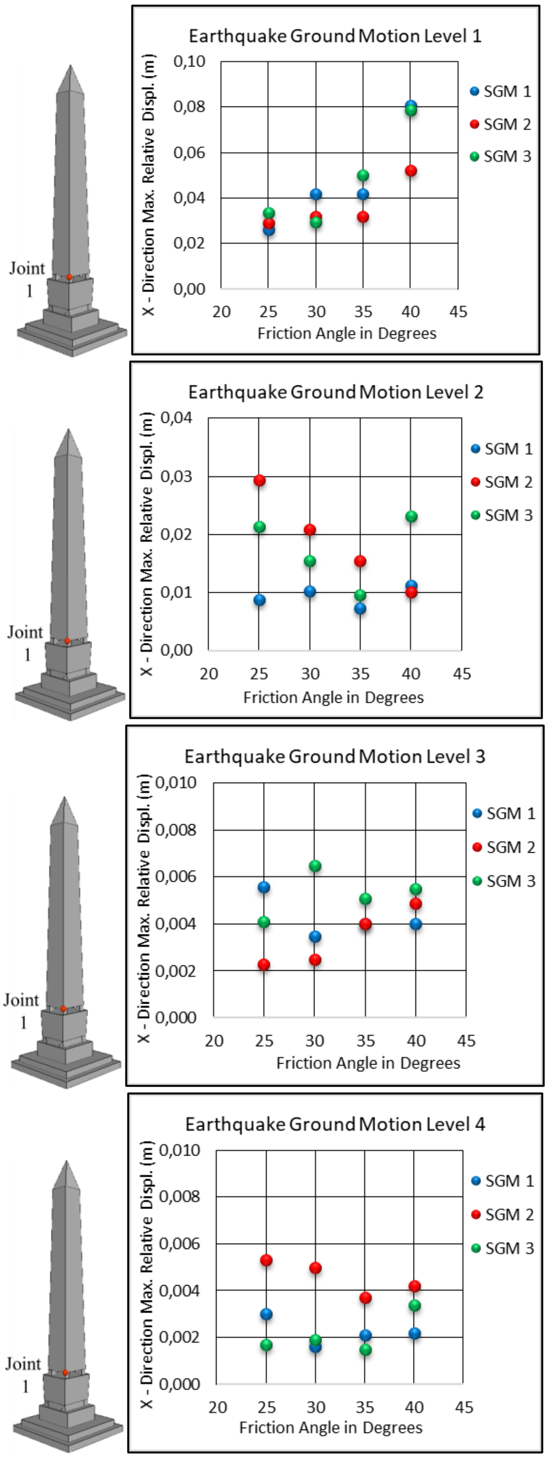

Fig. 10 The maximum relative displacement at Joint 1 calculated in terms of different friction angles under the three synthetic ground motion (SGM)

Obelisk and bronze cubes were monitored. Under real earthquakes the highest relative displacement of adjacent blocks take place between the Obelisk and bronze cubes under the synthetic ground motions (Joint 1).

The maximum displacement at the top of the Obelisk and the maximum relative displacement at the Joint 1 according to different friction angles calculated from the 1999 Kocaeli, Turkey and 1999 Düzce, Turkey earthquakes

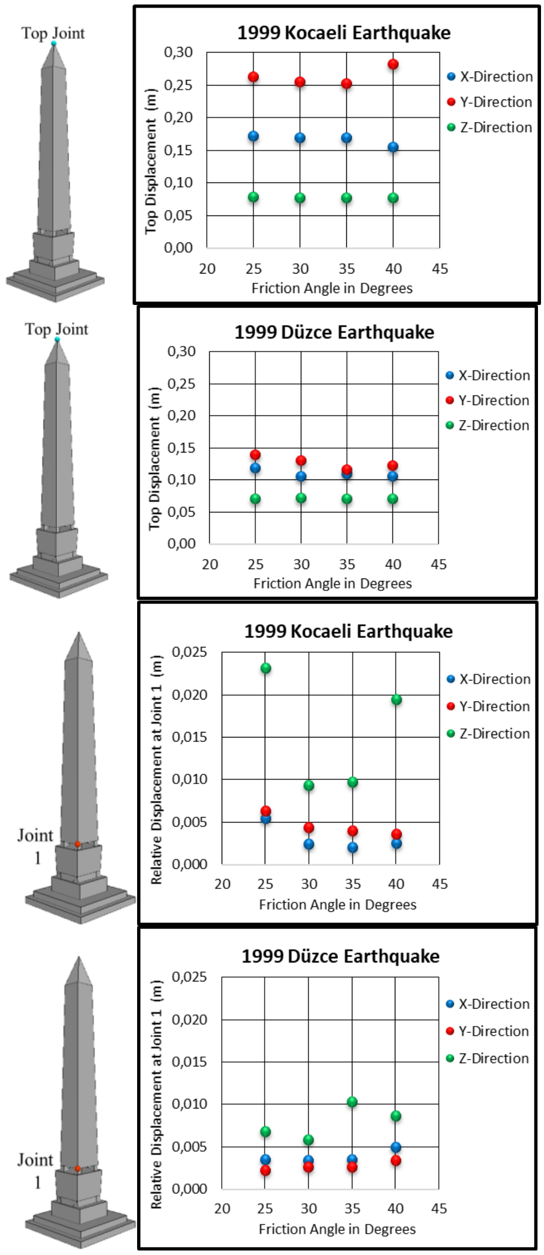

Fig. 11 The maximum displacement at the top of the Obelisk and the maximum relative displacement at the Joint 1 calculated using the 1999 Kocaeli, Turkey and 1999 Düzce, Turkey earthquakes in terms of different friction angles

are shown in Fig. 11. The Obelisk was experienced the maximum relative displacement in between the body and bronze cubes at the friction angle 25° and 40°. In case of the 1999 Kocaeli, Turkey earthquake, the maximum relative displacement in x direction vary between 0.025 and 0.055 cm which are very close that observed in *y* direction. Without collapse taking place, the top displacement for the 1999 Kocaeli, Turkey earthquake exceeds 0.28 cm in the *x* direction.

Besides, time-varying displacement histories at the top of the Obelisk for the 1999 Kocaeli and 1999 Düzce, Turkey earthquakes in three orthogonal direction are exhibited in Fig. 12 and also confirmed the results of the top

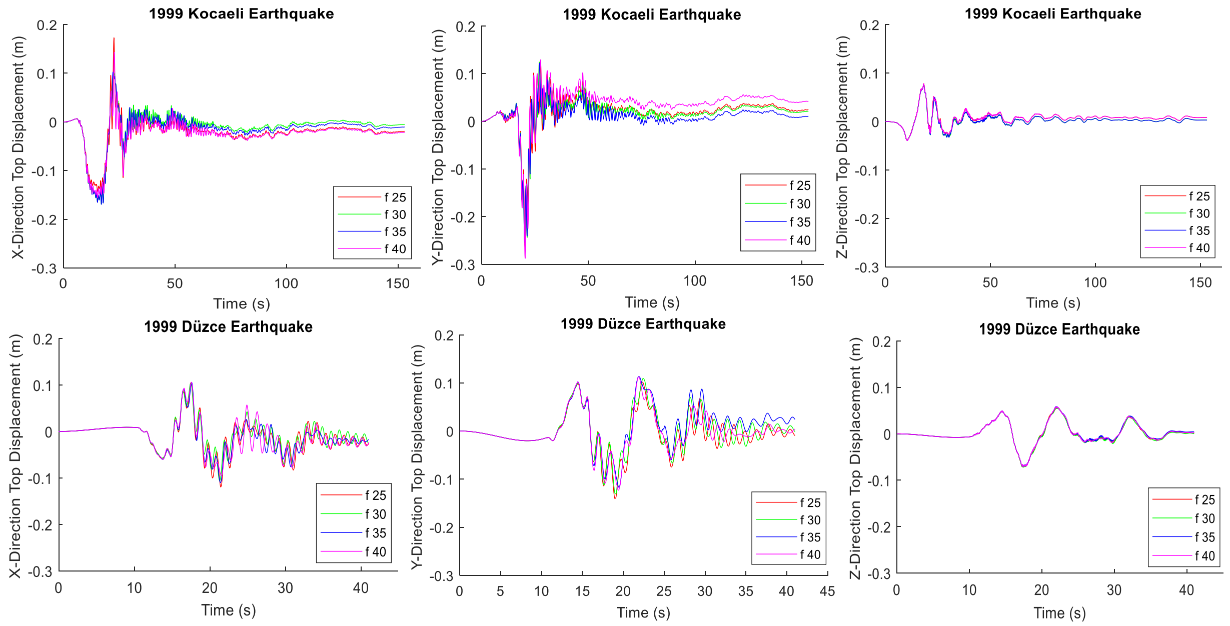

Fig. 12 Time varying displacement histories at the top of the Obelisk under the 1999 Kocaeli, and the 1999 Düzce, Turkey earthquakes

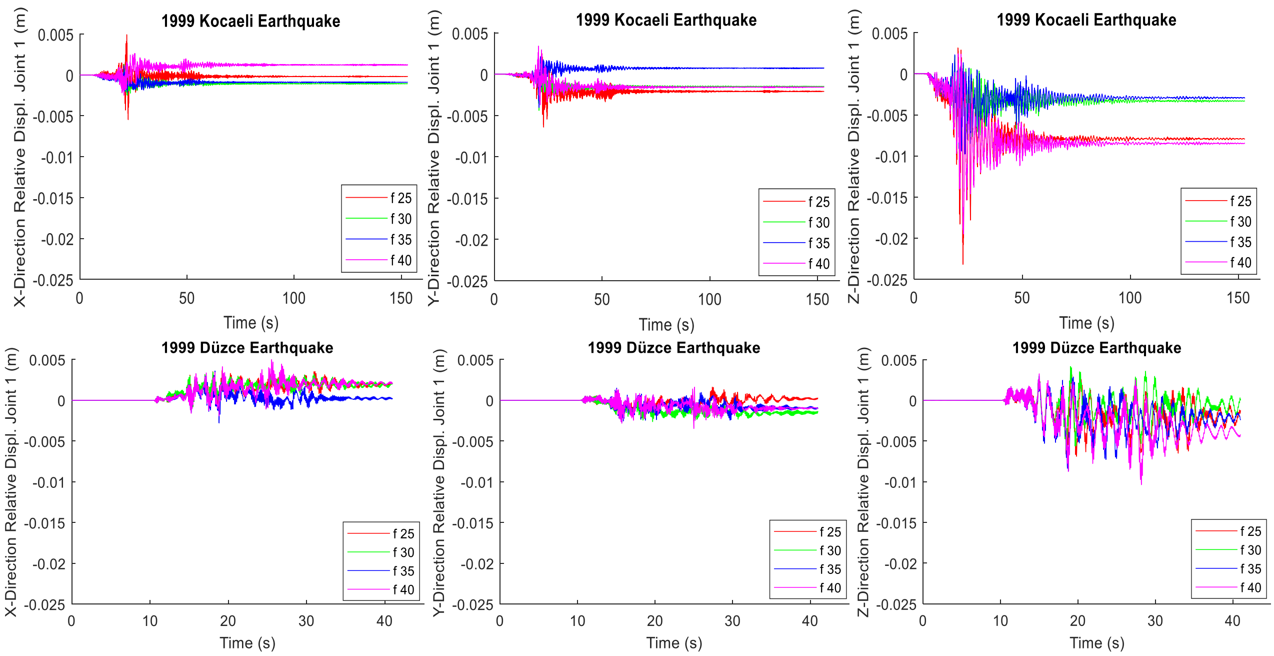

Fig. 13 The time varying relative displacement histories at the Joint 1 under the 1999 Kocaeli, and the 1999 Düzce, Turkey earthquakes

displacement in Fig. 13. As observed in Fig. 12, the friction angle between 25° and 40° produced the maximum displacement at the top of the Obelisk.

However, in the case of the 2010 Darfield, New Zealand earthquake, a collapse takes place at the friction angle of 25, 30 and 40 degrees. Sample images of notable damages and collapses are shown in Fig. 14. These images represent the state of the Obelisk during the seismic loading. They are valuable particularly to assess if the Obelisk has collapsed and whether the failure typology is local or global.

The top of the Obelisk has experienced displacements exceeding 180 cm in *x*-direction and 217 cm in *y*-direction without collapse under the 2010 Darfield, New Zealand earthquake at the friction angle of 35°. The Maximum top displacement observed in *z*-direction is 31 cm. Additionally, the permanent relative displacement (4 cm) between the Obelisk and bronze cubes are occurred under the 2010 Darfield, New Zealand earthquake at the friction angle of 35°.

Results show that horizontal sliding between the adjacent blocks of Obelisk and bronze cubes are non-negligible. Information about the structural behavior of the Obelisk was thus gained by considering the time-varying shear and normal stresses. Here, locations of stress

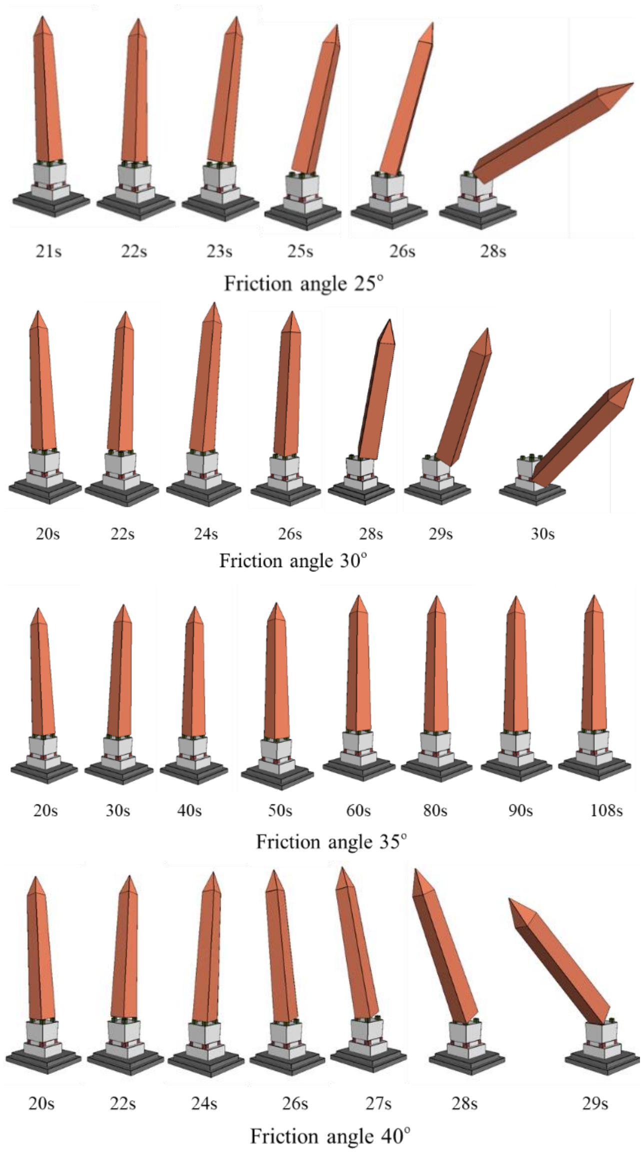

Fig. 14 The seismic behavior of the Obelisk under the 2010 Darfield, New Zealand earthquake for different friction angles between the Obelisk and bronze cube

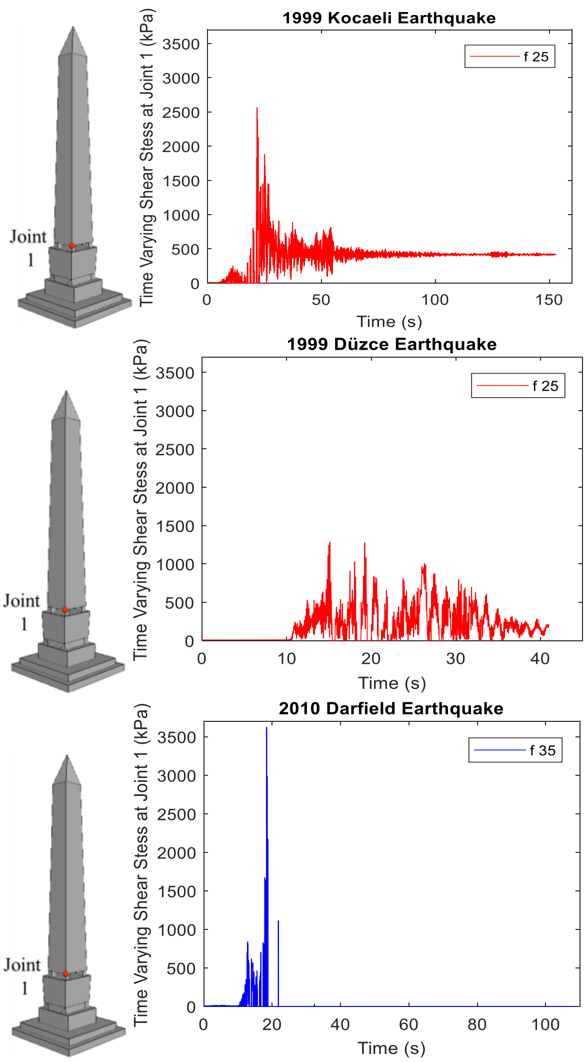

Fig. 15 At the friction angle of 25°, the time-varying shear stress histories under the 1999 Kocaeli, and 1999 Düzce, Turkey earthquakes and the 2010 Darfield earthquake responses

concentrations calculated were also evaluated.

Sample time-varying shear stress histories under the 1999 Kocaeli and 1999 Düzce, Turkey earthquakes at the friction angle of 25° and the 2010 Darfield earthquake responses are shown in Fig. 15.

Variations in the maximum shear and normal stresses were observed between the Obelisk and bronze cubes under real and synthetic time series. In the case of the 1999 Kocaeli, Turkey earthquake, the observed maximum shear at the friction angle of 25°, 30°, 35° and 40° is about 2500 kPa, 1000 kPa, 900 kPa and 1600 kPa, respectively. In the case of the 1999 Düzce earthquake, the Obelisk experienced the maximum variation of shear and normal stresses between the body and the bronze cubes at the friction angle of 25 and 40 in degrees. Synthetic time series for the ground motion level 2, 3, and 4 developed non-significant shear and normal stresses with respect to real earthquakes. This is probably due to the fact that, the numerical model subjected to synthetic ground motions only in one direction, the lower stresses occurred. Highest stresses were observed under the 2010 Darfield earthquake, which is best fitted with the target spectrum of ground motion level 1. As the amplitude of loading increases, the obelisk loses its potential energy and absorb inelastic energy, which is directly related to the level of damage.

6. Conclusions

The numerical studies reported in the paper show the effects of synthetic and real earthquakes on the Obelisk of Theodosius. The 3D numerical model of the Obelisk was constructed using the discrete element methodology. Variations in the displacement and the relative displacement of adjacent blocks in time were used to estimate the seismic behavior of the Obelisk in the past and the future.

From this study, the following conclusions can be drawn:

• According to the existing scanned data, the Obelisk does not have any significant inclination.
• The natural frequency of the principal mode of vibration of the obelisk studied is 0.886 Hz.
• The second bending mode of vibration and first torsional mode of vibration of the obelisk is 9.304 Hz and 10.75 Hz, respectively.
• According to the results observed from nonlinear dynamic analyses, the obelisk experienced the maximum top displacement under the 2010 Darfield, New Zealand earthquake and also the highest relative displacement of adjacent blocks between the Obelisk and bronze cubes at the friction angle of 25°, 30° and 40°.
• The 2010 Darfield, New Zealand earthquake which is well fit with the target spectrum of ground motion level 1 developed notable tensile stresses on the Obelisk.
The results indicated that the Obelisk could safely withstand the seismic load satisfy the earthquake ground motion that has a 50% probability to be exceeded in 50 years and 50% probability to be exceeded in 68 years.
• There is a possibility of overturning of the Obelisk under an earthquake ground motion with a return period of the 2475 year.
• The results from the records of variation of the relative displacement of the rigid blocks in time produced by dynamic analyses are evident to how the Obelisk of Theodosius survived from various important earthquakes near İstanbul for thousands of years.
• The response of the Obelisk in terms of the top displacement under the ground motion level 3 is almost the half of the response observed from the ground motion level 1.
• The effect of Level 1 ground shaking is 1.5 times of the effect of Level 2.
• This study shows that the DEM is a valuable tool to understand the dynamic response of Obelisks. During the analysis, the movements of blocks, their interactions with each other and contact forces are tracked because of being important in dynamic simulation.

Acknowledgments

I would like to gratefully acknowledge following institution and individuals. ITASCA for providing access to 3DEC; Emrullah Dar for his help with the total station recordings; Dr. Gülten Polat and Dr. Özlem Karagöz and for their comments to improve manuscript.

References

Abdel-Gawwad, A.K., El-Kady, H.M. and Shalaby, A.M. (2011), "Three dimensional dynamic analysis of ancient Egyptian obelisks to investigate their behavior under Aqaba earthquake", *J. Emerg. Trend. Eng. Appl. Sci. (JETEAS)*, **2**(2), 266-272.

Arslan, P.Y. (2016), "Towards a new honorific column: The column of Constantine in early Byzantine urban landscape", *METU J. Faculty Archit*., **33**(1), 121-145.

Barka, A.A. (1992), "The north Anatolian fault zone", *Annales Tectonicae*, **6**(Suppl), 164-195.

Bilen, C.A., Erisis, S., Er, S., Yilmaz, M., Angi, S. and Tugrul, A. (2016), "Deterioration types of stones used in Suleymaniye mosque (Istanbul, Turkey)", *IOP Conf. Series: Earth and Environmental Science*, **44**, Bristol, UK.

Bongiovanni, G., Clemente, P., Rinaldis, D. and Saitta, F. (2011), "Traffic-induced vibrations in historical buildings", *Proceedings of the 8th International Conference on Structural Dynamics, EURODYN 2011*, Leuven, Belgium, July.

Borghi, A., Angelici, D., Borla, M., Castelli, D., d'Atri, A. Gariani, G. Giudice, A. Lo., Martire, L., Re, A. and Vaggelli, G. (2015), "The stones of the statuary of the Egyptian Museum of Torino (Italy): Geologic and petrographic characterization", *Rendiconti Lincei*, **26**(4), 385-398.

Borghi, A., D'Amicone, E., Serra, M., Vaggelli, G. and Vigna, L. (2011), "Ramses II in majesty: A minero-petrographic and provenance rockstudy", *Proceedings of the 37th Int. Symp. on Archaeometry*, Ed. I. Turbanti-Memmi, Springer, Berlin, 193-198.

Çaktı, E., Saygılı, Ö., Lemos, J.V. and Oliveira, C.S. (2016), "Discrete element modeling of a scaled masonry structure and its validation", *Eng. Struct.*, **126**, 224-236.

Cundall, P.A. and Hart, R.D. (1992), "Numerical modeling of discontinua", *Eng. Comput*., **9**(2), 101-113.

Cundall, P.A. and Strack, O.D.L. (1979), "A discrete numerical model for granular assemblies", *Geotechnique*, **29**, 47-65.

Darwish, M. and Rashwan, M. (2018), "Structural dynamic characteristics of Ancient Egyptian obelisks and their responses to earthquake loads", *Pract. Period. Struct. Des. Constr*., **23**(2), 04018004

Engelbach, R. (1923), *The Problem of the Obelisks from A Study of the Unfinished Obelisk in Aswan*, T. Fisher Unwin Ltd., London.

Erdik, M. (2000), Report on 1999 Kocaeli and Düzce (Turkey) Earthquakes.

Geological (2007), Geotechnical Study Report According To The Construction Plans as a Result of Settlement Purposed Microzonation Works, Istanbul Metropolitan Municipalty Department Of Earthquake Risk Management And Urban Development Directorate Of Earthquake And Ground Analysis Istanbul.

Istanbul Metropolitan Municipality (IMM) (2007), "Geological-geotechnical study report according to the construction plans as a result of settlement purposed microzonation works".

Itasca (2016), 3DEC (3-Dimensional Distinct Element Code) Version 5.2, Itasca Consulting Group, Minneapolis, Minnesota.

Kelany, A., Negem, M., Tohami, A. and Heldal, T. (2009), "Granite quarry survey in the Aswan region, Egypt: Shedding new light on ancient quarrying", *Quarryscapes: Ancient stone quarry landscapes in the Eastern Mediterranean*, Eds. N. Abu-Jaber, E. Bloxam, P. Degryse, and T. Heldal, Geological Survey of Norway, Oslo.

Klemm, D.D. and Klemm, R. (2001), "The building stones of ancient Egypt-A gift of its geology", *J. Afr. Earth Sci*., **33**(3-4), 631-642.

Klemm, R. and Klemm, D. (2008), *Stones and Quarries in Ancient Egypt*, British Museum Press, London.

Lemos, J.V., Oliveira, C.S. and Navarro, M. (2015) "3-D nonlinear behavior of an obelisk subjected to the Lorca May 11, 2011 strong motion record", *Eng. Fail. Anal.*, **58**, 212-228.

Ludovico-Marques, M. (2008), "Contribution to the knowledge of the effect of crystallization of salts in the weathering of sandstones", Ph.D. Dissertation, Universidade Nova de Lisboa. Lisbon.

Mehrotra, A., Arede, A. and Dejong, M.J. (2015), "Discrete element modeling of a post-tensioned masonry arch", *Proceedings of The Fifteenth International Conference On Civil, Structural And Environmental Engineering Computing*,

Prague, Czech Republic, September.
Nakano, M., Citak, S.O. and Kalafat, D. (2015) "Focal mechanism determinations of earthquakes along the North Anatolian fault, beneath the Sea of Marmara and the Aegean Sea", *Earth, Plan. Space J.*, **67**, 159.
National Research Council (1982), *Conservation of Historic Stone Buildings and Monuments*, The National Academies Press, Washington, DC.
Polat, G., Özel, N.M. and Koulakov, I. (2016), "Investigating P- and S-wave velocity structure beneath the Marmara region (Turkey) and the surrounding area from local earthquake tomography", *Earth, Plan. Space Earth*, **68**, 132.
Pulatsu, B., Bretas, E.M. and Lourenco, P.B. (2016), "Discrete element modeling of masonry structures: Validation and application", *Geomech. Eng.*, **11**(4), 563-582.
Quigley, M.C., Van Dissen, R., Litchfield, N., Villamor, P., Duffy, B. Barrell, D., Furlong, K., Stahl, T., Bilderback, E. and Noble, D. (2012), "Surface rupture during the 2010 Mw 7.1 Darfield (Canterbury) earthquake: implications for fault rupture dynamics and seismic-hazard analysis", *Geology*, **40**, 5558.
Sadan, O.B., Bal, I.E. and Smyrou, E. (2007), "Structural analysis of Istanbul Beyazıt II Mosque retrofitted by Mımar Sınan, SHH'07", *International Symposium on Studies on Historical Heritage*, Antalya, Turkey.
Safran, L. (1993) "Points of view: the theodosian obelisk base in context", *Greek, Rom. Byzant. Stud.*, **34**, 409-435.
Şengör, A.M.C. and Yılmaz, Y. (1995), "Tethyan evolution of turkey: A plate tectonic approach", *Tectonophys.*, 181-241.
Taliercio, A. and Binda, L. (2007) "The Basilica of San Vitale in Ravenna: Investigation on the current structural faults and their mid-term evolution", *J. Cult. Herit.*, **8**, 99-118.
Vasconcelos, G. (2005), "Experimental Investigations on the mechanics of stone masonry: characterization of ancient granites and behavior of masonry shear walls", Ph.D. Dissertation, University of Minho.
Waters, M.J. (2016), "Reviving antiquity with granite: Spolia and the development of Roman Renaissance architecture", *Archit. Hist.*, **59**, 149-179.

CC